Brain Tumor Detection and Classification Using Adjusted InceptionV3, AlexNet, VGG16, VGG19 with ResNet50-152 CNN Model

Disha Sushant Wankhede[1]*,Chetan J.Shelke[2], Virendra Kumar Shrivastava[3], Rathnakar Achary[4], Sachi Nandan Mohanty[5]

[1,2,3,4] Department of Computer Science and Engineering, Alliance College of Engineering and Design, Alliance University,Bengaluru, Karnataka 562107

[5]School of Computer Science &Engineering, VIT-AP University Amaravati, India

Abstract

INTRODUCTION: Brain tumors have become a major global health concern, characterized by the abnormal growth of brain cells that can negatively affect surrounding tissues. These cells can either be malignant (cancerous) or benign (non-cancerous), with their impact varying based on their location, size and type.

OBJECTIVE: Early detection and classification of brain tumors are challenging due to their complex and variable structural makeup. Accurate early diagnosis is crucial to minimize mortality rates.

METHOD: To address this challenge, researchers proposed an optimized model based on Convolutional Neural Networks (CNNs) with transfer learning, utilizing architectures like Inception-V3, AlexNet, VGG16, and VGG19. This study evaluates the performance of these adjusted CNN models for brain tumor identification and classification using MRI data. The TCGA-LGG and The TCIA, two well-known open-source datasets, were employed to assess the model's performance. The optimized CNN architecture leveraged pre-trained weights from large image datasets through transfer learning.

RESULTS: The refined ResNet50-152 model demonstrated impressive performance metrics: for the non-tumor class, it achieved a precision of 0.98, recall of 0.95, F1 score of 0.93, and accuracy of 0.94; for the tumor class, it achieved a precision of 0.87, recall of 0.92, F1 score of 0.88, and accuracy of 0.96.

CONCLUSION: These results indicate that the refined CNN model significantly improves accuracy in classifying brain tumors from MRI scans, showcasing its potential for enhancing early diagnosis and treatment planning.

* Email: sdishaphd719@ced.alliance.edu.in

1. Introduction

The detection and categorization of brain tumors are vital for accurate diagnosis and effective treatment. Precise classification is crucial for timely detection, efficient treatment planning, and continuous monitoring of disease advancement.

Brain tumours can be categorized as either high-grade or low-grade. Gliomas, which include both high-grade and low-grade varieties, are a common type of brain tumor. The grading reflects the severity of the tumor, with tumors classified as either benign or malignant.

Deep learning techniques, particularly convolutional neural networks (CNNs), have become increasingly prevalent in medical imaging analysis. CNN models have shown considerable potential across a wide range of medical applications. One promising strategy for enhancing the efficacy and precision of CNN models in brain tumor identification and categorization is transfer learning. Transfer learning involves using a pre-trained model, often trained on a large dataset, as a starting point for training on a different, but related task. This model is then fine-tuned to identify and classify specific features pertinent to the new task.

According to Salama (2022), a study was conducted to categorize brain tumors using features extracted from low-quality images of 233 patients (Xin et al., 2021). The researchers employed a deep learning approach utilizing CNN classifiers initially designed for skin tumor classification. This method was adapted for brain tumor detection, resulting in a significant improvement in accuracy. In addition to transfer learning, deep unsupervised techniques within machine learning, such as autoencoders, can enhance CNN models. These methods are useful for various image analysis tasks, including reconstruction, image generation, and synthesis (Olut et al., 2018).

Active learning algorithms can also be employed to reduce labeling costs. These algorithms enable the model to select which samples to label, maximizing performance by strategic choice based on uncertainty or potential contribution to model improvement (Salama, 2022). This study proposes an adjusted CNN model using transfer learning for brain tumor detection and classification.

2. Literature Review

Vinoth, R et al. (2018) introduced a CNN-based method for tumor distinction. Rehman et al. (2020) employed a freezing approach to extract pattern properties from MRIs. Swati et al. (2019) suggested a fine-tuning strategy for classifying T1-weighted and contrast-enhanced magnetic resonance images, achieving an accuracy of 94.82%. Ahmed, K.B et al. (2017) explored deep learning and feature learning methods, pre-training a Deep CNN on a large dataset to estimate survival time, which showed an 81.8% success rate for the flare sequence. Asiri, A.A et al. (2022) noted that while neurons perform various tasks, some cells lose abilities, oppose each other, or develop malformations, potentially leading to benign or malignant brain tumors. Contributing factors include genetic changes, radiation exposure, and immune system issues.

Asiri, A.A et al. (2022) explained that the human brain is composed of numerous nerve tissues and intricate physical structures, controlling essential functions like senses, muscle development, and movement. Goding Sauer et al. (2019) summarized that although humanity has advanced in biomedical research, the cancerous expansion of nerve cells remains a challenge. Abiwinanda, N et al. (2019) differentiated between types of brain tumors, categorized as tumorous or non-tumorous. Tumors can be primary, originating in the brain, or secondary, having metastasized from elsewhere. Early detection and treatment are crucial.

Naseer, A. et al. (2020) stated that identifying brain tumors and predicting their progression remains challenging due to their complexity. Deep learning approaches offer better prediction and decision-making abilities. Ostrom, Q.T et al. (2018) noted that glioma, meningioma, and pituitary cancer are the most frequently diagnosed brain tumors. Meningioma originates from the membranes covering the brain and spinal cord, while glioma arises from glial cells supporting nerve cells. The pituitary gland affects several brain glands and physiological systems through its abnormal proliferation.

Long, J et al. (2015) and Balaji, C et al. (2023) worked on object identification, categorization, and feature extraction using deep learning techniques. Cheng, J et al. (2015) utilized a series of two-dimensional images collected from hospitals in China between 2005 and 2020. Table 1 summarizes the connected work.

Table 1. Summary of similar work

Reference	Algorithm	No. of Images	Limitations	DataSet Used	Accuracy %
Chetana Srinivas et al. [26][40]	VGG -16 with fine tuning	233	Increased computational cost Large storage space is necessary	TCGA, BraTS	94.82
Second B. Defeng Wang et al.[33]	(L1 -SVM (MLPC)	285	Necrotic and non-enhancing tumor regions combined with an enhanced tumor region	TCGA, BraTS	0.97
Kelvin K. Wong , et al.[32][34][35]	deep learning	492	Input permutation feature/ to extract prognostic differential expressed genes	TCGA	0.96
Saima Rathore, et al.[31]	Deep learning, Computational pathology	663	Extracted from ex-vivo digital pathology	TCGA	0.88
Sebastian R. van der Voort, et al.[29]	SVM	284	Decision-making on treatment.	TCIA	0.81
Stephen Bacchi et al.[28]	CNN	255	This task may be assisted by deep learning (DL)	TCGA,GBM	0.82

3. Methods

Researchers proposed a CNN model utilizing Inception-V3, CNN-AlexNet, as well as the VGG16 and VGG19 networks. Table 2 presents description of dataset used in this work.

3.1 Dataset Explanation

Table 2. Datasets description

Sr.No	DataSet Name	Patients	MRI Images	Type of disease
1	TCGA and TCIA	110	15090	Glioma Brain Tumor
2	Figshare	233	21390	Glioma Brain Tumor
3	Kaggle	80	10288	Glioma Brain Tumor

Figshare dataset is a collection of T1-weighted 3064 contrast-enhanced pictures of brain tumors of 233 patients, including 768 slices [11]. The TCGA and TCIA datasets consist of data from 110 patients [12].

For this research, the imaging dataset was downloaded from the Imaging Archive. An MRI dataset, freely available on kaggle.com, was used to test the models. MRI scans are essential for identifying brain tumors, thus MRI images were used to validate model performance and accuracy. Each MRI image was resized to 512 pixels horizontally and vertically. In this analysis, 80% of the images were used for training, and 20% for testing. Samples of MRI images with corresponding masks are presented in Figure 1.
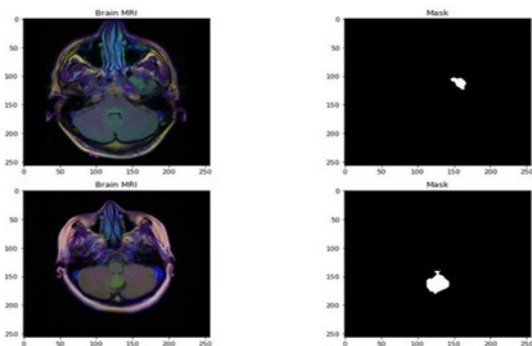
Fig.1: Image samples with corresponding masks

3.2. CNN Model

For tumor prediction, the CNN model does not consider the masks; it solely depends on MRI scans. The convolution layers are typically the first layer, abstracting the images using filters. Each filter's response to the input image is represented by a set of features [17].

The second layer, known as pooling, is added to the feature map to reduce size while maintaining key features. This reduction is performed with fewer parameters to prevent overfitting. The compressed output from both layers is then fed into fully connected layers for feature extraction, and a threshold applied to the output of the CNN to determine the presence or absence of a tumor.
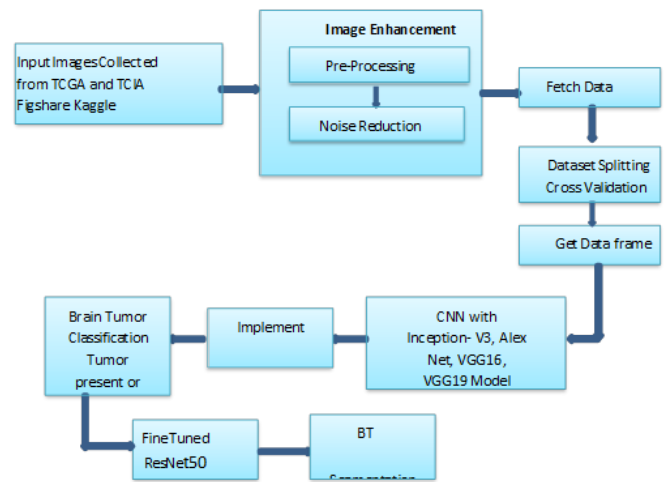
Fig. 2: Proposed model architecture

Figure 2 illustrates this process, which depends on the convolutional layer. This layer utilizes various filters to extract relevant features. The output and size of the given layer are calculated using Equations (1) and (2), respectively:

$$AB_{ab} = \Delta(C_{ab} - D_L + Y_i) \tag{1}$$

where AB_{ab} is the feature map, Δ is the activation function, D_L is the input width and $C_{i\epsilon f}L, Y_{i\epsilon f}$ are filter (f) channels.

$$\text{size} = \frac{in - filter\_size}{strid} + 1 \tag{2}$$

The pooling layer accomplishes various tasks, including maximum, minimum, and average pooling [18]. The most widely used pooling function is the Max Pooling (MP) Layer.

Equations (3) and (4) describe the pooling layer and its output, where "o" represents the output and "PL" stands for the pooling region.

$$PLi,=maxpl,o\epsilon R. \qquad (3)$$

Pooling Layer out size = $\dfrac{Convolution\_Layer - Pooling\_Size}{Stride}$ (4)

The final step is fine-tuning. In order to enhance performance, the ResNet50 model [37] has been loaded with pre-trained weights from extensive datasets. ResNet50, a convolutional neural network (CNN) model with 50 layers is known for its depth and ability to learn intricate features from images. By leveraging pre-trained weights, the model benefits from prior training, which helps it achieve better performance on new tasks.

Although the fine-tuning strategy applied to ResNet50 only marginally improves accuracy, it is a critical step in adapting the model to the specific requirements of brain tumor detection and classification. The detailed description of each layer in ResNet50, which contributes to its high performance, is presented in Table 3.

Additionally, Figure 3 provides a visual representation of the generalized CNN model, illustrating its layered structure and workflow. This comprehensive setup underscores the importance of each layer in achieving accurate and reliable results in medical imaging tasks.
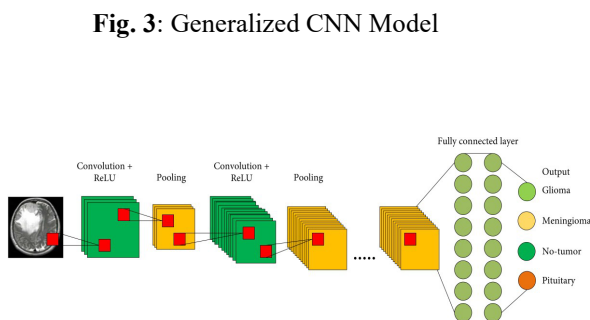
CNN Layer	Description
Input_Image	Takes image channels as inputs and transforms the image
Convolutional_Layer	An important component of CNN which extracts features
Batch Normalization	Enhances the network by normalizing input values to have zero mean and unit variance
ReLU_Function	Input values include nonlinear functions that zero all negative and odd values
Pooling_Layer	Used after each convolutional layer in CNNs to reduce overfitting, manage parameters, and adjust for each layer. There are three types: minimum, maximum, and average pooling.
Softmax_Function	A CNN begins with an initial value derived from the pooled and convolutional layers.
Fully_Connected_Layer	As all the inputs are fed into the final layer, this layer connects to all the neurons of NN to perform the actual classification.
Classification_Layer	In this layer, class entropy loss values are computed and, ultimately, the classes are matched with their appropriate categories.

Table 3. CNN layers description

3.2.1 CNN Inception V3 Model

A detailed outline of the Inception V3 model is presented in Table 4 which uses forty-two layers.

Fig. 3: Generalized CNN Model

Inception V3 Layer Type	Patch / stride size	Input Size
Convolution_Layer(CL)	3×3/2	299×299×3
CL	3×3/1	149×149×32
CL padded	3×3/1	147×147×32
Pool	3×3/2	147×147×64
CL	3×3/1	73×73×64
CL	3×3/2	71×71×80
CL	3×3/1	35×35×192
3 × Inception	Module 1	35×35×288
5 × Inception	Module 2	17×17×768
2 × Inception	Module 3	8×8×1280
Pool Layer	8 × 8	8 × 8 × 2048
Linear Function	Logits	1 × 1 × 2048
Softmax_Function	Classifier	1 × 1 × 1000

Table 4. CNN Inception V3 Layers Description

3.2.2 CNN AlexNet Model

In the AlexNet architecture, variable kernel sizes are employed in the initial convolution layer and the subsequent multiple layers (ML) layers. This strategic use of different kernel sizes allows the network to capture a wider range of features from the input images. To process and eliminate the characteristics of vectors, fully connected (FC) layers are employed, specifically FC6, the first fully connected layer, and FC7, the second fully connected layer, are used in activation.

The AlexNet CNN architecture includes a substantial feature extraction capacity, with each of the fully connected layers, FC6 and FC7, containing 4096 vector features.
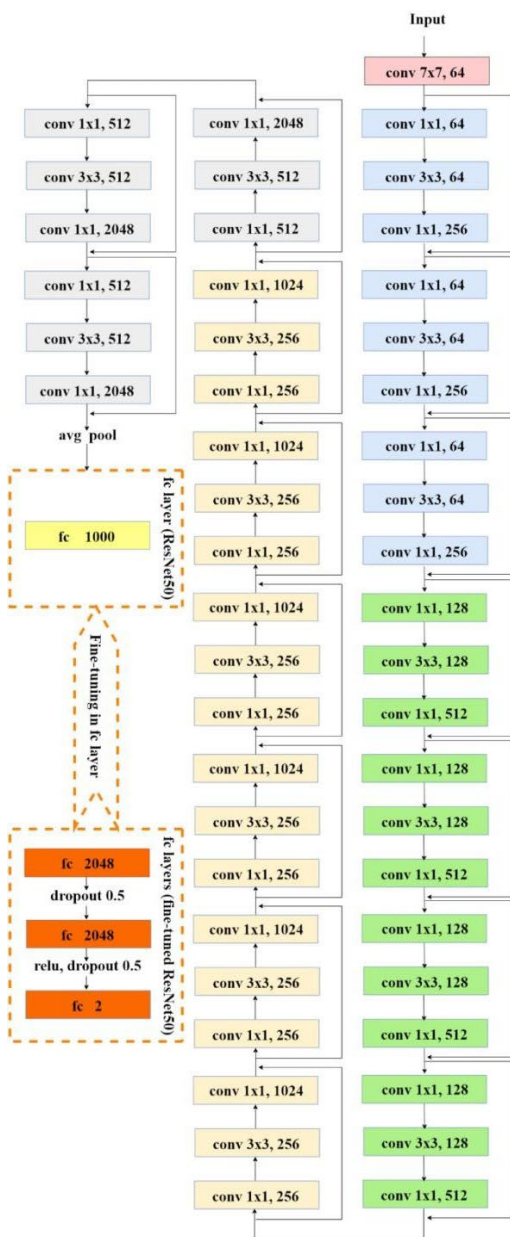
Fig.4: AlexNet50 Model

3.2.3 CNN VGG16 Model

The architecture of VGG16 and VGG19 is characterized by its structured approach, comprising 5 sets of convolutional layers, each followed by a MaxPool operation.

VGG16 consists of 16 layers, while VGG19 extends this with 19 layers. These convolutional layers are cascaded in increasing depth across the sets, enhancing the network's ability to learn hierarchical features from input images.

For a detailed breakdown of the layers in VGG16 and VGG19, refer to Table 5 and Table 6 respectively, which provide comprehensive descriptions of the convolutional and pooling layers within each set, highlighting their pivotal role in feature extraction and spatial downsampling.

Table 5. CNN VGG16 Layers description

Layer		Feature map	Size	Kernel Size	Stride	Activation
Input	Image1	1	224x224x 3	-	-	-
1	2 X Convolution	64	224x224 x64	3x3	1	
2	MP Layer	64	112x112 x 64	==	2	relu
3	2 X Convolution	128	112x112 x 128	==	1	==
4	MP Layer	128	56 x 56 x 128	==	2	==
5	2 X Convolution	256	56 x 56 x 256	==	1	==
6	MP Layer	256	28 x 28 x 256	==	2	==
7	3 X Convolution	512	28x28 x 512	==	1	==
8	MP Layer	512	14x14 x 512	==	2	==
9	3 X Convolution	512	14x14 x 512	==	1	==
10	MP Layer	512	7x7x512	==	2	==
11	FC	512	25088	==	1	==
12	FC	512	4096	==	2	==
13	FC	512	4096	==	1	==
O/P	FC	512	1000	==	2	Softmax

3.2.4 CNN VGG19 Model

Table 6. CNN VGG19 layers description

Layer		Feature map	Size	Kernel Size	Stride	Activation
Input	Image1	1	224x224x3	-	-	-
1	conv3	64	224x224 x64	3x3	1	
2	MP Layer	64	112x112 x 64	==	2	relu
3	conv3	128	112x112 x 128	==	1	==
4	MP Layer	128	56 x 56 x 128	==	2	==
5	conv3	256	56 x 56 x 256	==	1	==
6	MP Layer	256	28 x 28 x 256	==	2	==
7	conv3	512	28x28 x 512	==	1	==
8	MP Layer	512	14x14 x 512	==	2	==
9	conv3	512	14x14 x 512	==	1	==
10	MP Layer	512	7x7x512	==	2	==
11	FC	512	4096	==	1	==
12	FC	512	4096	==	2	==
13	FC	512	4096	==	1	==
O/P	FC	512	1000	==	2	Soft Max

3.3. Fine Tune Residual network (ResNet) 50-152 model stage

The model updates its layer weights by employing back propagation and stochastic gradient descent. This enables the model to make a conclusive judgment regarding the presence or absence of tumors by establishing a threshold on the computed probability.

During the training phase detailed in Table 7, the enhanced ResNet50-152 model, integrated with convolutional neural networks (CNN), learns to differentiate brain MRI data and categorize them into tumor and healthy classes. Modifications are made to the final layers of the ResNet50 model by introducing new fully connected layers specifically designed for brain tumor detection and classification.

Subsequently, the entire model undergoes fine-tuning using a new dataset of MRI brain scans. This fine-tuning process involves adjusting the weights of all model layers, refining

their ability to distinguish tumor characteristics from healthy tissue.

The MRI scans undergo preprocessing to enhance contrast between tumors and surrounding tissues, ensuring more accurate feature extraction by the model. Once fine-tuned, the model produces a probability distribution indicating the likelihood of tumor presence. A predefined threshold is then applied to this probability distribution to make the final diagnosis.

By leveraging the robust features learned from the pre-trained ResNet50, this method achieves high accuracy in detecting and classifying brain tumors using MRI scans. Fine-tuning the model with specialized data further enhances its ability to perform this critical diagnostic task effectively.

Table 7. Fine-tune ResNet50-152 layers description

Layer	Output	18 layer	34 layer	50 layer	101 layer	152 layer
Conv1	112x112			7x7, 64, stride 2		
Conv2	56 x 56			3x3 max pool, stride 2		
Conv3	28 x 28	$\begin{bmatrix}3x3,64\\3x3,64\end{bmatrix}$x2 $\begin{bmatrix}3x3,128\\3x3,128\end{bmatrix}$x2	$\begin{bmatrix}3x3,64\\3x3,64\end{bmatrix}$x3 $\begin{bmatrix}3x3,128\\3x3,128\end{bmatrix}$x4	$\begin{bmatrix}1x1,64\\3x3,64\\1x1,256\end{bmatrix}$x3 $\begin{bmatrix}1x1,128\\3x3,128\\1x1,512\end{bmatrix}$x4	$\begin{bmatrix}1x1,64\\3x3,64\\1x1,256\end{bmatrix}$x3 $\begin{bmatrix}1x1,128\\3x3,128\\1x1,512\end{bmatrix}$x4	$\begin{bmatrix}1x1,64\\3x3,64\\1x1,256\end{bmatrix}$x3 $\begin{bmatrix}1x1,128\\3x3,128\\1x1,512\end{bmatrix}$x8
Conv4	14 x 14	$\begin{bmatrix}3x3,256\\3x3,256\end{bmatrix}$x2	$\begin{bmatrix}3x3,256\\3x3,256\end{bmatrix}$x6	$\begin{bmatrix}1x1,256\\3x3,256\\1x1,1024\end{bmatrix}$x6	$\begin{bmatrix}1x1,256\\3x3,256\\1x1,1024\end{bmatrix}$x23	$\begin{bmatrix}1x1,256\\3x3,256\\1x1,1024\end{bmatrix}$x36
Conv5	7 x 7	$\begin{bmatrix}3x3,256\\3x3,256\end{bmatrix}$x2	$\begin{bmatrix}3x3,256\\3x3,256\end{bmatrix}$x3	$\begin{bmatrix}1x1,512\\3x3,512\\1x1,2028\end{bmatrix}$x3	$\begin{bmatrix}1x1,512\\3x3,512\\1x1,2028\end{bmatrix}$x3	$\begin{bmatrix}1x1,512\\3x3,512\\1x1,2028\end{bmatrix}$x3
	1 x 1			1x1 average pool, 1000-d fc, softmax		

4. Results

Brain tumor identification, classification, and segmentation are accomplished through the integration of convolutional neural networks (CNNs) such as Inception-V3, CNN-AlexNet, VGG16, and VGG19 models, along with a custom-tailored ResNet50-152 layers model. This approach enhances overall accuracy by leveraging the strengths of each individual model.

4.1. CNN with Inception-V3, CNN-AlexNet , VGG16,VGG19 Model Results

In this study, CNN architectures were employed for the diagnosis of brain tumors. The models achieved significant performance metrics, making them robust tools for tumor detection. The CNN models using Inception-V3, CNN-AlexNet, VGG16, and VGG19 demonstrated an accuracy of 92%. Figure 3 illustrates accuracy and loss trends represented by red and blue lines. Precision, averaging between 90% and 94%, indicates high reliability in correctly identifying tumors. Similarly, recall values ranged between 83% and 97%, reflecting the model's ability to detect most positive cases accurately. The F1 score, averaging between 0.88 and 0.93 as shown in Table 8, underscores the models' effectiveness in balancing precision and recall metrics.

EAI

Table 8. CNN model with InceptionV3, AlexNet, VGG16, VGG19.

	Precision		Recall		F1 Score	Accu-racy	Exec. Time
	Non-tumor	Tumor	Non-tum.	Tum.	Non-tumor	Non-tum./Tum.	
Inception-v3	0.90	0.94	0.97	0.83	0.93	0.92	1.75
AlexNet	0.91	0.94	0.96	0.82	0.92	0.91	2.55
VGG16	0.91	0.95	0.95	0.85	0.92	0.93	2.83
VGG19	0.92	0.95	0.97	0.85	0.93	0.93	2.70
Fine-Tuned ResNet50-152 layer	0.93	0.96	0.98	0.87	0.95	0.94	0.88

Fig.5: Accuracy

Accuracy
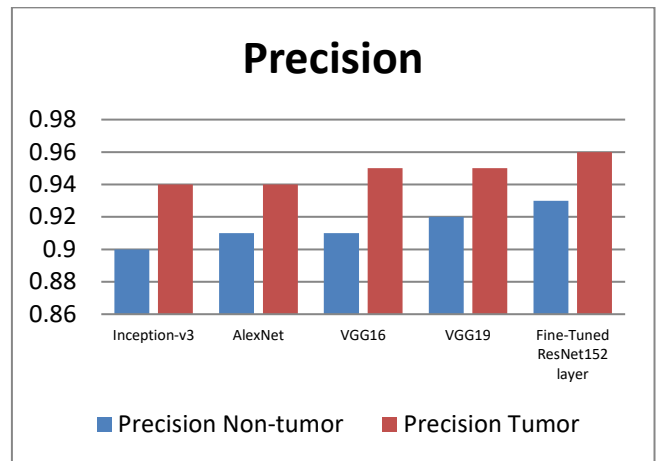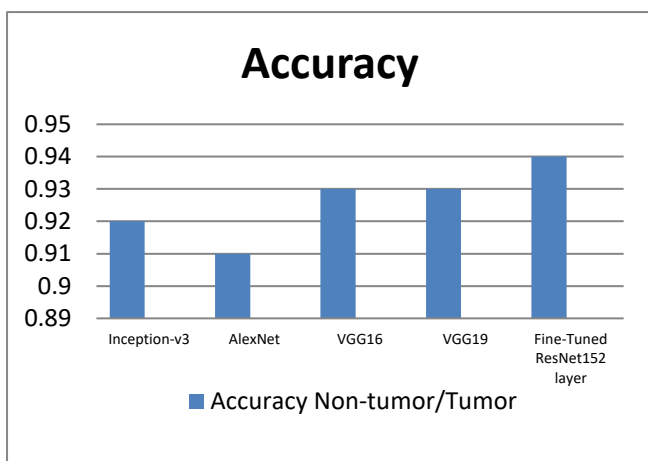
Precision

Fig.6. Precision
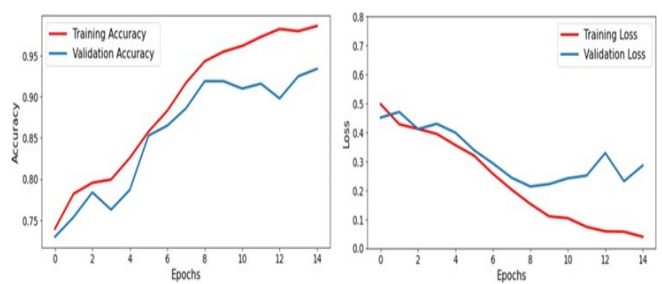
Fig.7. Accuracy and loss graph combined all CNN Mode

4.2.   ResNet50-152 Model

The proposed approach utilized CNN models including Inception-V3, AlexNet, VGG16, and VGG19 alongside a customized ResNet50-152 architecture for the classification of brain tumors. The dataset comprised images depicting both tumors and non-tumors, which were used to train the models. The ResNet50 model achieved high accuracy, typically around 94%. Figure 8 illustrates accuracy and validation loss. Precision, which assesses the ratio of correctly classified positive tumor cases to all positive predictions, was also high. Recall, indicating the proportion of correctly classified tumor cases among all actual tumor cases, ranged between 87% and 98%. The F1 score, a measure balancing precision and recall, typically ranged between 0.92 and 0.95, as depicted in Figure 8.
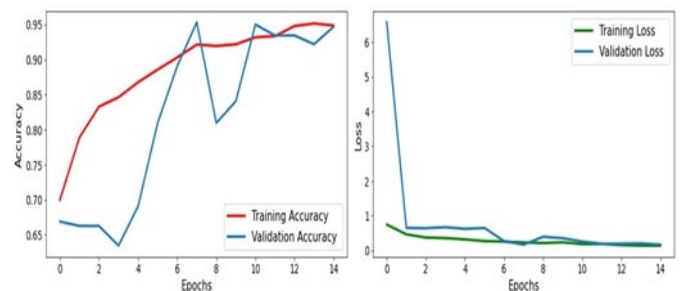
Fig.8. Accuracy and loss graph ResNet50-152 layer Model

5. Conclusions

The proposed approach integrates CNN models such as InceptionV3 with a fine-tuned ResNet50-152 layer to achieve high accuracy by leveraging the strengths of both architectures. Specifically, the study focused on brain tumor identification through MRI scans using the optimized ResNet50-152 layer architecture. Compared to the baseline CNN model, the adjusted ResNet50-152 model demonstrated superior performance. It achieved precision of 0.98, recall of 0.95, F1 score of 0.93, and accuracy of 0.94 for non-tumor cases, and precision of 0.87, recall of 0.92, F1 score of 0.88, and accuracy of 0.96 for tumor cases. These results indicate that the CNN model with the refined ResNet50-152 layer outperforms traditional CNN models in accurately detecting and categorizing brain tumors from MRI data.

References

1.   Asiri, A.A.; Aamir, M.; Shaf, A.; Ali, T.; Zeeshan, M.; Irfan, M.; Alshamrani, K.A.; Alshamrani, H.A.; Alqahtani, F.F.; Alshehri, A.H.D. Block-Wise Neural Network for Brain Tumor Identification in Magnetic Resonance Images. Comput. Mater. Contin. 2022, 73, 5735–5753.

2.   Asiri, A.A.; Shaf, A.; Ali, T.; Aamir, M.; Usman, A.; Irfan, M.; Alshamrani, H.A.; Mehdar, K.M.; Alshehri, O.M.; Alqhtani, S.M. Multi-Level Deep Generative Adversarial Networks for Brain Tumor Classification on Magnetic Resonance Images. Intell. Autom. Soft Comput. 2023, 36, 127–143.

3.   Asiri, A.A.; Ali, T.; Shaf, A.; Aamir, M.; Shoaib, M.; Irfan, M.; Alshamrani, H.A.; Alqahtani, F.F.; Alshehri, O.M. A Novel Inherited Modeling Structure of Automatic Brain Tumor Segmentation from MRI. Comput. Mater. Contin. 2022, 73, 3983–4002

4.   Goding Sauer, A.; Siegel, R.L.; Jemal, A.; Fedewa, S.A. Current prevalence of major cancer risk factors and screening test use in the United States: Disparities by education and race/ethnicity. Cancer Epidemiol. Prev. Biomark. 2019, 28, 629–642.

5.   Siegel, R.L.; Miller, K.D.; Jemal, A. Cancer statistics, 2015. CA Cancer J. Clin. 2015, 65, 5–29.

6.   Abiwinanda, N.; Hanif, M.; Hesaputra, S.T.; Handayani, A.; Mengko, T.R. Brain tumor classification using convolutional neural network. In Proceedings of the World Congress on Medical Physics and Biomedical Engineering 2018, Prague, Czech Republic, 3–8 June 2018; Springer: Singapore, 2019.

7.   Naseer, A.; Rani, M.; Naz, S.; Razzak, M.I.; Imran, M.; Xu, G. Refining Parkinson's neurological disorder identification through deep transfer learning. Neural Comput. Appl. 2020, 32, 839–854.

8.   Ostrom, Q.T.; Gittleman, H.; Truitt, G.; Boscia, A.; Kruchko, C.; Barnholtz-Sloan, J.S. CBTRUS Statistical report: Primary brain and other central nervous system tumors diagnosed in the United States in 2011–2015. Neuro. Oncol. 2018, 20 (Suppl. S4), iv1–Abir, T.A.; Siraji, J.A.; Ahmed, E.; Khulna, B. Analysis of a novel MRI based brain tumour classification using probabilistic neural network (PNN). Int. J. Sci. Res. Sci. Eng. Technol. 2018, 4, 65–79.

9.   Naseer, A.; Rani, M.; Naz, S.; Razzak, M.I.; Imran, M.; Xu, G. Refining Parkinson's neurological disorder identification through deep transfer learning. Neural Comput. Appl. 2020, 32, 839–854.

10.   Long, J.; Shelhamer, E.; Darrell, T. Fully convolutional networks for semantic segmentation. In Proceedings of the IEEE Conference on Computer Vision and Pattern Recognition, Boston, MA, USA, 7–12 June 2015.

11.   Cheng, J. Brain Tumor Dataset. Figshare. Dataset. 2017. Available online: https://figshare.com/articles/braintumordataset/1512427 (accessed on 27 January 2022).

12.   Pedano, N.; Flanders, A.E.; Scarpace, L.; Mikkelsen, T.; Eschbacher, J.M.; Hermes, B.; Sisneros, V.; Barnholtz-Sloan, J.; Ostrom, Q. Radiology Data from The Cancer Genome Atlas Low Grade Glioma [TCGA-LGG] collection. Cancer Imaging Arch. 2016.

13.   Clark, K.; Vendt, B.; Smith, K.; Freymann, J.; Kirby, J.; Koppel, P.; Moore, S.; Phillips, S.; Maffitt, D.; Pringle, M.; et al. The Cancer Imaging Archive (TCIA): Maintaining and operating a public information repository. J. Digit. Imaging 2013, 26, 1045–1057.

14.   Cheng, Jun (2017). brain tumor dataset. figshare. Dataset. https://doi.org/10.6084/m9.figshare.1512427.v5

15.   Sartaj. Brain Tumor Classification Dataset. Available online: https://www.kaggle.com/datasets/sartajbhuvaji/brain-tumor- classification-mri (accessed on 2 May 2023).

16.   Nickparvar, M. Brain Tumor Classification Dataset. Available online: https://www.kaggle.com/datasets/masoudnickparvar/brain- tumor-mri-dataset (accessed on 2 May 2023)

17.   Aamir, M.; Ali, T.; Shaf, A.; Irfan, M.; Saleem, M.Q. ML-DCNNet: Multi-level deep convolutional neural network for facial expression recognition and intensity estimation. Arab. J. Sci. Eng. 2020, 45, 10605–10620.

18.   Jie, H.J.; Wanda, P. RunPool: A dynamic pooling layer for convolution neural network. Int. J. Comput. Intell. Syst. 2020, 13, 66–76.

19.   Vinoth, R.; Venkatesh, C. Segmentation and Detection of Tumor in MRI images Using CNN and SVM Classification. In Proceedings of the 2018 Conference on Emerging Devices and Smart Systems (ICEDSS), Tiruchengode, India, 2–3 March 2018; IEEE: Piscataway,

NJ, USA, 2018.

20. Rehman, A.; Naz, S.; Razzak, M.I.; Akram, F.; Imran, M. A deep learning-based framework for automatic brain tumors classification using transfer learning. Circuits Syst. Signal Process. 2020, 39, 757–775

21. Swati, Z.N.K.; Zhao, Q.; Kabir, M.; Ali, F.; Ali, Z.; Ahmed, S.; Lu, J. Brain tumor classification for MR images using transfer learning and fine-tuning. Comput. Med. Imaging Graph. 2019, 75, 34–46.

22. Ahmed, K.B.; Hall, L.O.; Goldgof, D.B.; Liu, R.; Gatenby, R.A. Fine-tuning convolutional deep features for MRI based brain tumor classification. In Proceedings of the Medical Imaging 2017: Computer-Aided Diagnosis, Orlando, FL, USA, 3 March 2017; SPIE: Bellingham, WA, USA, 2017.

23. Balaji, C. ., & Veni, S. . (2023). Automatic Skull Stripping from MRI of Human Brain using Deep Learning Framework for the Diagnosis of Brain Related Diseases. International Journal of Intelligent Systems and Applications in Engineering, 11(4), 439–445. Retrieved from: https://ijisae.org/index.php/IJISAE/article/view/3541

24. Meenakshi Sooda, Shruti Jainb*, Jyotsna Dograc.(2023) Classification and Pathologic Diagnosis of Gliomas in MR Brain Images , International Conference on Machine Learning and Data Engineering ScienceDirect comProcedia Computer Science 218 (2023) 706– 717

25. Seyedamid Seyedhashemi, Mehdi Esmaeili. Detecting Tumors in MRI Scans using a Convolutional Neural Network. Authorea. February 22, 2023.

26. Chetana Srinivas, Nandini Prasad K. S., Mohammed Zakariah, Yousef Ajmi Alothaibi Kamran Shaukat, B. Partibane, and Halifa Awal (2022) Deep Transfer Learning Approaches in Performance Analysis of Brain Tumor Classification Using MRI Images, Wearable Devices for Smart Healthcare

27. Chen SC, Lo CM, Wang SH, Su EC. RNA editing-based classification of diffuse gliomas: predicting isocitrate dehydrogenase mutation and chromosome 1p/19q codeletion. BMC Bioinformatics. 2019 Dec 24;20 (Suppl 19):659. doi: 10.1186/s12859-019-3236-0. PMID: 31870275; PMCID: PMC6929429.

28. Bacchi S, Zerner T, Dongas J, Asahina AT, Abou-Hamden A, Otto S, Oakden-Rayner L, Patel S. Deep learning in the detection of high-grade glioma recurrence using multiple MRI sequences: A pilot study. J Clin Neurosci. 2019 Dec;70:11-13. doi: 10.1016/j.jocn.2019.10.003. Epub 2019 Oct 21. PMID: 31648967.

29. Sebastian R. van der Voort; Fatih Incekara; Predicting the 1p/19q Codeletion Status of Presumed Low-Grade Glioma with an Externally Validated Machine Learning Algorithm Clin Cancer Res (2019) 25 (24): 7455–7462. https://doi.org/10.1158/1078- 0432.CCR-19-1127

30. Bangalore Yogananda CG, Shah BR, Vejdani-Jahromi M, Nalawade SS, Murugesan GK, Yu FF, Pinho MC, Wagner BC, Mickey B, Patel TR, Fei B, Madhuranthakam AJ, Maldjian JA. A novel fully automated MRI-based deep-learning method for classification of IDH mutation status in brain gliomas. Neuro Oncol. 2020 Mar 5;22(3):402-411. doi: 10.1093/neuonc/noz199. Retraction in: Neuro Oncol. 2023 Jun 2;25(6):1197. PMID: 31637430; PMCID: PMC7442388.

31. Saima Rathore, Muhammad Aksam Iftikhar, Zissimos Mourelatos, Prediction of overall survival and molecular markers in gliomas via analysis of digital pathology images using deep learning, Image and Video Processing, https://doi.org/10.48550/arXiv.1909.09124

32. Wong KK, Rostomily R, Wong STC. Prognostic Gene Discovery in Glioblastoma Patients using Deep Learning. Cancers (Basel). 2019 Jan 8;11(1):53. doi: 10.3390/cancers11010053. PMID: 30626092; PMCID: PMC6356839.

33. Chen C, Zheng A, Ou X, Wang J, Ma X. Comparison of Radiomics-Based Machine-Learning Classifiers in Diagnosis of Glioblastoma from Primary Central Nervous System Lymphoma. Front Oncol. 2020 Sep 15;10:1151. doi: 10.3389/fonc.2020.01151. PMID: 33042784; PMCID: PMC7522159.

34. Shrivastava, V. K., Shelke, C. J., Shrivastava, A., Mohanty, S. N., & Sharma, N. (2023). Optimized Deep Learning Model for Disease Prediction in Potato Leaves. EAI Endorsed Transactions on Pervasive Health and Technology, 9.

35. Karnik, M.P., Kodavade, D.V. (2023),Abstractive Summarization with Efficient Transformer Based Approach , International Journal on Recent and Innovation Trends in Computing and Communication, ISSN: 2321-8169 Volume: 11 Issue: 4 DOI: https://doi.org/10.17762/ijritcc.v11i4.6454

36. Karnik, M.P., Kodavade, D.V. (2023). A Survey on Controllable Abstractive Text Summarization. In: Abraham, A., Pllana, S., Casalino, G., Ma, K., Bajaj, A. (eds) Intelligent Systems Design and Applications. ISDA 2022. Lecture Notes in Networks and Systems, vol 715. Springer, Cham. https://doi.org/10.1007/978-3-031-35507-3_30

37. Shrivastava, V. K., Shrivastava, A., Sharma, N., Mohanty, S. N., & Pattanaik, C. R. (2023). Deep learning model for temperature prediction: A case study in New Delhi. Journal of Forecasting.

38. Wankhede, D.S., Shelke, C.J. (2023). An Investigative Approach on the Prediction of Isocitrate Dehydrogenase (IDH1) Mutations and Co-deletion of 1p19q in Glioma Brain Tumors. In: Abraham, A., Pllana,

S., Casalino, G., Ma, K., Bajaj, A. (eds) Intelligent Systems Design and Applications. ISDA 2022. Lecture Notes in Networks and Systems, vol 715. Springer, Cham. https://doi.org/10.1007/978- 3-031-35507-3_19

39.   Wankhede, D.S., Pandit, S., Metangale, N., Patre, R., Kulkarni, S., Minaj, K.A. (2022). Survey on Analyzing Tongue Images to Predict the Organ Affected. In: Hybrid Intelligent Systems. HIS 2021. Lecture Notes in Networks and Systems, vol 420. Springer, Cham. https://doi.org/10.1007/978-3-030-96305-7_56

40. S. Solanki, U. P. Singh, S. S. Chouhan and S. Jain, "Brain Tumor Detection and Classification Using Intelligence Techniques: An Overview," in IEEE Access, vol. 11, pp. 12870-12886, 2023, doi: 10.1109/ACCESS.2023.3242666.

41.   G. S. Prasad and V. S. Gaikwad, "A survey on user awareness of cloud security", Int. J. of Engineering and Technology, vol. 7, no. 2.32, pp. 131-135, May 2018.

42.   Gudapati S.P., Gaikwad V. (2021) Light-Weight Key Establishment Mechanism for Secure Communication Between IoT Devices and Cloud. In: Satapathy S., Bhateja V., Janakiramaiah B., Chen YW. (eds) Intelligent System Design. Advances in Intelligent Systems and Computing, vol 1171. Springer, Singapore. https://doi.org/10.1007/978-981-15-5400-1_55

43.   A. Shetty, A. Thorat, R. Singru, M. Shigawan and V. Gaikwad, "Predict Socio-Economic Status of an Area from Satellite Image Using Deep Learning," 2020 International Conference on Electronics and Sustainable Communication Systems (ICESC), 2020, pp. 177-182,
doi: 10.1109/ICESC48915.2020.9155696.

44.   Shrimant, Gaikwad Vidya, Ravindranath, K. & Prasad, Gudapati Syam (2023) A mathematical model for secure Cloud-IoT communication: Introducing the revolutionary lightweight key mechanism, Journal of Discrete Mathematical Sciences and Cryptography, 26:5, 1341–1354, DOI: 10.47974/JDMSC-1750

45.   Shrivastava, V. K., Shrivastava, A., Sharma, N., Mohanty, S. N., & Pattanaik, C. R. (2023). Deep learning model for temperature prediction: an empirical study. Modeling Earth Systems and Environment, 9(2), 2067-2080.

46.   Batra, R., Mahajan, M., Shrivastava, V. K., & Goel, A. K. (2021). Detection of COVID-19 using textual clinical data: a machine learning approach. Impact of AI and data science in response to coronavirus pandemic, 97-109.

47.   Saini, V., Rai, N., Sharma, N., & Shrivastava, V. K. (2022, December). A Convolutional Neural Network Based Prediction Model for Classification of Skin Cancer Images. In International Conference on Intelligent Systems and Machine Learning (pp. 92-102). Cham: Springer Nature Switzerland.

48.   Singhal, A., Phogat, M., Kumar, D., Kumar, A., Dahiya, M., & Shrivastava, V. K. (2022). Study of deep learning techniques for medical image analysis: A review. Materials Today: Proceedings, 56, 209-214.

49.   Shrivastava, V. K., Kumar, A., Shrivastava, A., Tiwari, A., Thiru, K., & Batra, R. (2021, August). Study and trend prediction of Covid-19 cases in India using deep learning techniques. In Journal of Physics: Conference Series (Vol. 1950, No. 1, p. 012084). IOP Publishing.

50.   Batra, R., Shrivastava, V. K., & Goel, A. K. (2021). Anomaly Detection over SDN Using Machine Learning and Deep Learning for Securing Smart City. In Green Internet of Things for Smart Cities